RESEARCH ARTICLE

Direct Target Network of the *Neurospora crassa* Plant Cell Wall Deconstruction Regulators CLR-1, CLR-2, and XLR-1

James P. Craig,[a,b,c] Samuel T. Coradetti,[a,b,d] Trevor L. Starr,[a,b,e] N. Louise Glass[a,b]

Department of Plant and Microbial Biology, University of California, Berkeley, Berkeley, California, USA[a]; Energy Biosciences Institute, University of California, Berkeley, Berkeley, California, USA[b]; Chan Soon-Shiong Institute of Molecular Medicine, Windber, Pennsylvania, USA[c]; Buck Institute for Research on Aging, Novato, California, USA[d]; Dupont Industrial Biosciences, Palo Alto, California, USA[e]

ABSTRACT **Fungal deconstruction of the plant cell requires a complex orchestration of a wide array of intracellular and extracellular enzymes. In *Neurospora crassa*, CLR-1, CLR-2, and XLR-1 have been identified as key transcription factors regulating plant cell wall degradation in response to soluble sugars. The XLR-1 regulon was defined using a constitutively active mutant allele, resulting in hemicellulase gene expression and secretion under noninducing conditions. To define genes directly regulated by CLR-1, CLR-2, and XLR-1, we performed chromatin immunoprecipitation and next-generation sequencing (ChIPseq) on epitope-tagged constructs of these three transcription factors. When *N. crassa* is exposed to plant cell wall material, CLR-1, CLR-2, and XLR-1 individually bind to the promoters of the most strongly induced genes in their respective regulons. These include promoters of genes encoding cellulases for CLR-1 and CLR-2 (CLR-1/CLR-2) and promoters of genes encoding hemicellulases for XLR-1. CLR-1 bound to its regulon under noninducing conditions; however, this binding alone did not translate into gene expression and enzyme secretion. Motif analysis of the bound genes revealed conserved DNA binding motifs, with the CLR-2 motif matching that of its closest paralog in *Saccharomyces cerevisiae*, Gal4p. Coimmunoprecipitation studies showed that CLR-1 and CLR-2 act in a homocomplex but not as a CLR-1/CLR-2 heterocomplex.**

IMPORTANCE **Understanding fungal regulation of complex plant cell wall deconstruction pathways in response to multiple environmental signals via interconnected transcriptional circuits provides insight into fungus/plant interactions and eukaryotic nutrient sensing. Coordinated optimization of these regulatory networks is likely required for optimal microbial enzyme production.**

Received 28 August 2015 **Accepted** 3 September 2015 **Published** 13 October 2015

Citation Craig JP, Coradetti ST, Starr TL, Glass NL. 2015. Direct target network of the *Neurospora crassa* plant cell wall deconstruction regulators CLR-1, CLR-2, and XLR-1. mBio 6(5):e01452-15. doi:10.1128/mBio.01452-15.

Editor B. Gillian Turgeon, Cornell University

Address correspondence to N. Louise Glass, Lglass@berkeley.edu.

This article is a direct contribution from a Fellow of the American Academy of Microbiology.

Filamentous fungi play an important role in the carbon cycle by degrading plant biomass. Plant cell wall deconstruction by filamentous fungi requires the ability to efficiently secrete large quantities of lignocellulolytic enzymes, a trait which has been harnessed by the biofuel industry for conversion of plant biomass to simple sugars that can be subsequently synthesized into fuel molecules (1). However, lignocellulose enzyme production remains a major expense (2) and a contributor to the carbon footprint (3) of next-generation biofuels.

In the wild, the niche of the filamentous fungus *Neurospora crassa* is the decomposition of recently burned plant material (4, 5). Recent work in *N. crassa* identified a set of genes that were differentially expressed on the three main components of plant carbohydrates: cellulose, hemicellulose, and pectin (6–8). The transcription factors CLR-1 (NCU07705) and CLR-2 (NCU08042) were identified as essential for growth on cellulose (6, 9), while a third transcription factor, XLR-1 (NCU06971), was shown to be necessary for growth on hemicellulose but not cellulose (8).

These three transcription factors are well conserved across filamentous ascomycete species (6, 10–14). Orthologs of *xlr-1* are required for both cellulase and hemicellulase gene expression in *Aspergillus niger*, *A. oryzae*, and *Trichoderma reesei* (11, 12, 14) but are required only for hemicellulase gene expression in *N. crassa*, *Fusarium oxysporum*, *A. nidulans*, and *Magnaporthe grisea* (10, 15, 16). Orthologs of *clr-2* are required for cellulase expression in *N. crassa*, *A. nidulans*, *A. oryzae*, and *Penicillium oxalicum* (9, 13) but not in *T. reesei* (17). In *N. crassa*, the CLR-1 and CLR-2 (CLR-1/CLR-2) regulon is composed of ~212 genes (6, 9), while the XLR-1 regulon is composed of ~245 genes (8); regulons reflect both direct and indirect targets of these transcription factors. To further characterize the plant cell wall deconstruction regulatory network, we combined chromatin immunoprecipitation and next-generation sequencing (ChIPseq) with RNA sequencing (RNAseq) to determine the direct target gene regulons of CLR-1, CLR-2, and XLR-1 under conditions of exposure to different plant biomass components. To this end, we developed a *xlr-1* mutant that showed constitutive activity under noninducing conditions and characterized the XLR-1 regulon. Direct target genes of CLR-1, CLR-2, and XLR-1 included those encoding proteins

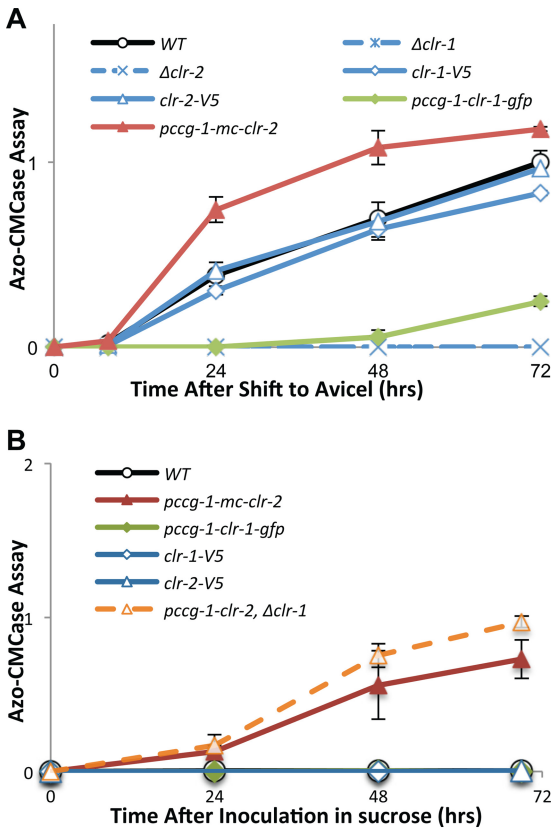

FIG 1 Comparison of activity and secreted protein levels for strains carrying differently tagged and regulated *clr-1* and *clr-2* constructs compared to the wild-type parental strain and the Δ*clr-1* and Δ*clr-2* deletion strains. (A) Endoglucanase activity after a switch of sucrose cultures to media with Avicel as the sole carbon source. (B) Endoglucanase activity with sucrose as the sole carbon source. Activity in panels A and B was normalized to wild-type Avicel cultures from panel A.

known to be involved in plant biomass deconstruction or utilization but also genes encoding hypothetical proteins, uncharacterized transporters, and transcription factors. DNA binding motifs for CLR-1, CLR-2, and XLR-1 were identified, and physical interactions of CLR-1 and CLR-2 were explored. This in-depth study illuminated the regulation and interactions of genes/proteins involved in plant biomass degradation and provided hypotheses that will help guide the optimization of pathways for increased enzyme production in filamentous fungi.

RESULTS

CLR-1 target gene regulon. We first tested how variants of CLR-1 (including epitope tags, promoter sequences, and genome localization) affected chromatin immunoprecipitation-sequencing (ChIPseq) results. One strain contained a C-terminal green fluorescent protein (GFP)-tagged *clr-1* allele regulated by the promoter from the clock-controlled-gene-1 (p*ccg-1-clr-1-gfp*) strain, which is constitutively active under these experimental conditions (18), and integrated into the *his-3* locus in a Δ*clr-1* deletion strain. A second *clr-1* strain carried the smaller V5 epitope at the C terminus integrated at the resident *clr-1* locus, thus preserving the native *clr-1* promoter (*clr-1-V5*). The p*ccg-1-clr-1-gfp* strain had reduced endoglucanase activity, while the *clr-1-V5* strain had wild-type (WT) enzyme activity and protein secretion (Fig. 1A). The control Δ*clr-1* strain showed no enzyme activity or protein secretion. Constitutive expression of *clr-1-gfp* via the *ccg-1* promoter under sucrose conditions yielded no detectable enzyme activity; under these conditions, *ccg-1* drives expression of downstream genes at higher levels than the *clr-1* native promoter, even under conditions of cellulose (Avicel) exposure. These data indicate that the presence of CLR-1 under noninducing conditions was insufficient for induction of a cellulolytic response (Fig. 1B).

To define target promoters bound by CLR-1, we performed ChIPseq on *clr-1-gfp* and *clr-1-V5* strain cultures switched to Avicel for 4 h, a condition that strongly induces lignocelluloytic genes (6, 19). A strain carrying cytosolic GFP under the regulation of the p*ccg-1* promoter was used as a control for normalization (see Materials and Methods). Comparison of the CLR-1-GFP and CLR-1-V5 libraries showed that 93% of the top 500 CLR-1-V5 binding sites overlapped with at least one of the CLR-1-GFP libraries (see Fig. S1 in the supplemental material). CLR-1-V5 peaks without a corresponding peak in the CLR-1-GFP libraries were characterized by lower fold enrichment, were located within nonpromoter regions, or had high background levels obscuring the signal. These results indicate that there was not a bias between the GFP and V5 epitopes and that promoter differences of the tagged *clr-1* genes did not play a significant role in ChIPseq results.

Under Avicel conditions, CLR-1 was significantly enriched at 203 promoter regions representing 293 genes due to the presence of binding sites located in the promoter regions of 90 divergently transcribed genes. CLR-1 gene targets included 16 predicted glycosyl hydrolases, including the major exoglucanases encoded by *cbh-1*, *gh6-2*, and *gh6-3* (20) (see Dataset S1 in the supplemental material). CLR-1 also bound at locations upstream of 8 putative transporter genes, including *cdt-2* (21) and the cellobionic acid transporter gene *cbt-1* (22, 23) and 6 transcription factor genes, including *clr-2*, *xlr-1*, *vib-1* (all implicated in cellulase or hemicellulase regulation) (6, 8, 24, 25), *cpc-1* (regulation of amino acid metabolism) (26, 27), a homolog to *tamA* (nitrogen metabolism) (28), the circadian rhythm modulator gene *frq*, and NCU03184, which contains a zinc finger domain.

The binding profiles of CLR-1-GFP under sucrose versus cellulose (Avicel) conditions showed a large degree of overlap, with 68% of the Avicel-bound promoters also being bound under sucrose conditions (see Dataset S1 in the supplemental material). CLR-1 binding signals on sucrose were generally weaker than on Avicel, although many highly bound promoters on Avicel completely lacked signal on sucrose. Genes that exhibited Avicel-specific binding (see Dataset S1) included those encoding cellulases (*cbh-1*, *gh6-2*, *gh5-1*, *gh61-4*, *gh2-2*, *gh11-2*, *gh55-1*, and *gh74-1*), transporters (*cbt-1* and NCU11342), and xylose reductase (*xyr-1*). To validate our ChIPseq results, we conducted targeted ChIP-quantitative PCR (qPCR) experiments using four genes: *gh6-3*, *cbh-1*, *gh6-2*, and *gh61-4*. In keeping with our ChIPseq data, the ChIP-qPCR experiments showed that enrichment of CLR-1-GFP and CLR-1-V5 under Avicel conditions was more prominent at the promoters of *gh6-3* and *cbh-1* and less prominent at the promoters of *gh6-2* and *gh61-4* (see Fig. S2). ChIP-qPCR of CLR-1-GFP on sucrose also mirrored the ChIPseq data, with enrichment at the *gh6-3* promoter but not at the *cbh-1*, *gh6-2*, or *gh61-4* promoter, confirming their Avicel-specific binding patterns (see Fig. S2). These results also showed that CLR-1 was competent to bind the promoters of target genes, including

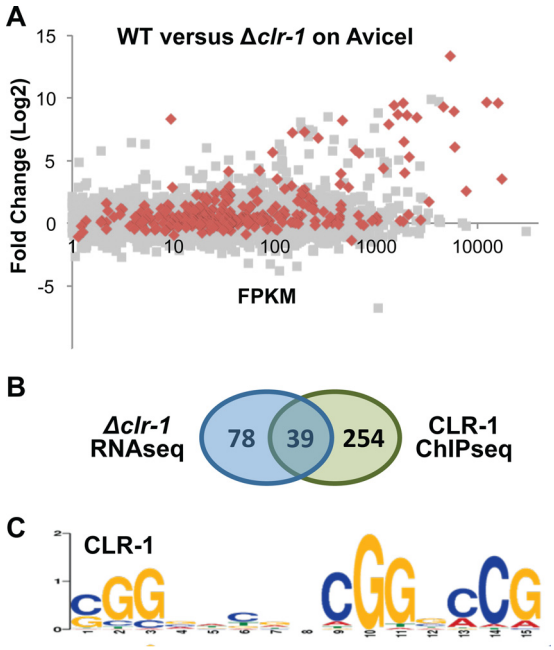

FIG 2 Concordance of CLR-1 ChIPseq enrichment with differential expression of genes that require CLR-1 for induction. (A) Fold change in gene expression of the wild-type parental strain (FGSC 2489) versus the Δ*clr-1* mutant on Avicel. Genes with significant binding in ChIP experiments are shown in red. (B) Venn diagram showing overlap of genes differentially expressed in the WT versus Δ*clr-1* strain under Avicel conditions (Cuffdiff; Padj = <0.05; 4-fold) and genes with significant binding by CLR-1 within their promoter regions. (C) Consensus binding site based on promoter regions bound by CLR-1.

the promoter of *clr-2* (see below), under sucrose conditions, although cellulase activity was not detectable under these conditions.

We then compared the ChIPseq and RNAseq datasets to identify genes that showed a correlation between binding by CLR-1 and dependence on CLR-1 for expression (6) (see Dataset S2 in the supplemental material). The results of our analysis revealed 39 such genes (Fig. 2A and B and Table 1). These genes encoded eighteen enzymes predicted to be involved in plant cell wall deconstruction, as well as two sugar transporters (encoded by *cdt-1* and NCU11342), plus the cellulose degradation regulator encoded by *clr-2*. Twelve genes that encoded proteins with predicted enzyme domains but whose potential role in plant cell wall deconstruction was unclear were also bound and regulated by CLR-1. Six additional genes encoded hypothetical proteins or contained domains of unknown biochemical function (DUF and HET). The highly expressed endoxylanase NCU07225 and transporter *cdt-2* genes, while not identified as significantly differentially expressed by our strict criteria, were both bound by CLR-1 and showed expression levels that were modulated 5-fold and 11-fold, respectively. By assessing motifs found within the 203 promoter regions bound by CLR-1, a highly enriched motif (CGGN5CGGNCCG) located in ~50% of the peaks was identified (Fig. 2C) (*E* value, $1.9E^{-73}$), with the highest probability for the motif found at the center of the peak.

CLR-2 target gene regulon. Constitutive expression of *clr-1* in media lacking a cellulolytic inducer did not result in cellulase activity (Fig. 1B). In contrast, constitutive expression of *clr-2* under noninducing conditions results in robust cellulolytic activity (9). These observations suggest fundamental differences between the regulatory mechanisms of CLR-1 and CLR-2. To better understand these differences, we performed ChIPseq on a strain containing N-terminally tagged mCherry-*clr-2* that was regulated by the *ccg-1* promoter and resided at the *his-3* locus (*mc-clr-2*) (9). The *mc-clr-2* strain grew normally on sucrose and showed robust growth on Avicel, with higher cellulase activity and protein secretion than the wild-type parental strain (Fig. 1A), which is consistent with previous observations (9).

The ChIPseq libraries from the *mc-clr-2* strain grown on Avicel were normalized to a cytosolic mCherry ChIPseq library (see Materials and Methods). CLR-2 bound to 114 promoter sites upstream of 164 genes (see Dataset S1 in the supplemental material). As described above for CLR-1, we compared the MC-CLR-2 ChIPseq data set with the constitutively expressed *clr-2* RNAseq

TABLE 1 Genes upregulated and differentially expressed in the wild-type strain versus a Δ*clr-1* strain and whose promoter region was bound by CLR-1

NCU no.	Locus	Annotation or domain
NCU00130	*gh1-1*	Intracellular β-glucosidase
NCU00206[a]	*cdh-1*	Cellobiose dehydrogenase
NCU00326		Calcium homeostasis protein
NCU00762[a]	*gh5-1*	Glycosylhydrolase family 5
NCU00801[a]	*cdt-1*	Cellodextrin transporter
NCU00836[a]	*gh61-7*	Polysaccharide monooxygenase (AA9 family)
NCU01050[a]	*gh61-4*	Polysaccharide monooxygenase (AA9 family)
NCU01059	*gh47-3*	Glycosyl hydrolase family 47 (alpha mannosidase)
NCU01944		Hypothetical protein
NCU02240[a]	*gh61-1*	Polysaccharide monooxygenase (AA9 family)
NCU02485		AMP-binding domain
NCU02915[a]		RhoGAP domain
NCU02916[a]	*gh61-3*	Polysaccharide monooxygenase (AA9 family)
NCU05057[a]	*gh7-1*	Endoglucanase
NCU05574		Acetyltransferase domain
NCU05846[a]		Domain of unknown function DUF1479
NCU05863		ATPase (AAA) domain
NCU05864[a]		Hypothetical protein
NCU05955[a]	*gh74-1*	Cel74a; xyloglucanase
NCU06704		Ribosome-associated membrane protein RAMP4
NCU07190[a]	*gh6-3*	Glycosylhydrolase family 6
NCU07339[a,b]		Hypothetical protein
NCU07340[a,b]	*cbh-1*	Cellobiohydrolase
NCU07487	*gh3-6*	Periplasmic β-glucosidase
NCU07897[a,b]		HET domain
NCU07898[a,b]	*gh61-13*	Polysaccharide monooxygenase (AA9 family)
NCU08042	*clr-2*	Transcription factor
NCU08115	*msh3*	DNA mismatch repair protein
NCU08412[a]		Endo-β-1,4-mannanase
NCU08750		Isoamyl alcohol oxidase
NCU08755	*gh3-3*	Secreted β-glucosidase
NCU08784		Short-chain dehydrogenase domain
NCU09505		Alpha/beta hydrolase domain
NCU09523[a,b]		Hypothetical protein
NCU09524[a,b]		Cellulose binding domain
NCU09680[a]	*gh6-2*	Glycosylhydrolase family 6
NCU09689		Alpha/beta hydrolase domain
NCU09764	*gh61-14*	Polysaccharide monooxygenase (AA9 family)
NCU11342		MFS hexose transporter

[a] NCU numbers in bold represent promoter regions of genes bound by both CLR-1 and CLR-2.

[b] Promoter regions of genes (NCU numbers) bound by CLR-1 that may regulate 2 genes in opposite orientations.

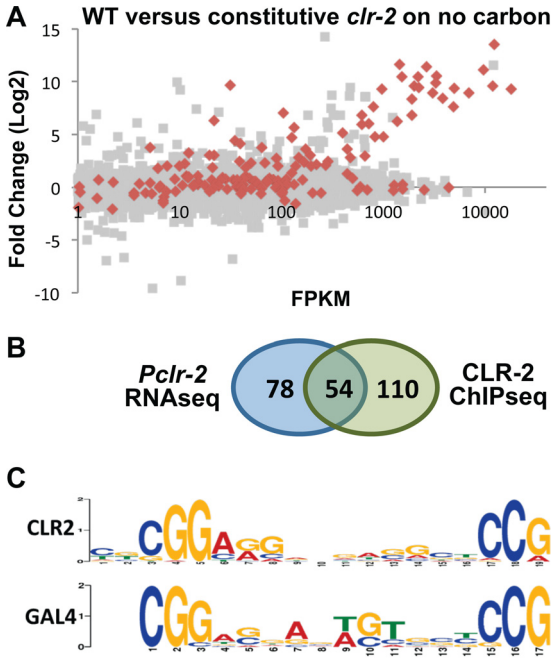

FIG 3 Concordance of CLR-2 ChIPseq enrichment with differential expression of genes that require CLR-2 for induction. (A) Fold change in gene expression in a *clr-2* constitutive expression strain versus the wild-type parental strain exposed to no-carbon conditions (4 h). Genes with significant binding by CLR-2 in ChIPseq experiments are shown in red. (B) Venn diagram showing overlap of genes differentially expressed under no-carbon conditions in the *clr-2* constitutive expression strain (Cuffdiff; Padj = <0.05; 4-fold) and genes with significant binding by CLR-2 in their promoter regions. (C) Consensus binding site for CLR-2 compared to Gal4p.

data set to find genes that exhibited a correlation between binding by CLR-2 and dependence on CLR-2 for expression (Fig. 3A and B; see also Dataset S2) (6, 9). The results of this analysis included 37 predicted carbohydrate active enzymes (all major cellulases and lytic polysaccharide monooxygenases [LPMOs], as well as some major hemicellulases), 4 carbohydrate esterases, and the enzyme encoded by *cdh-1*; two transporters, encoded by *cdt-1* and *cdt-2*; six transcription factors, four of which, including those encoded by *xlr-1*, *col-26*, *sah-2*, and *hac-1*, have known effects on cellulase/hemicellulase production (8, 24, 29–31); two predicted transcription factors with no known function (encoded by NCU04855 and NCU03184); and two enzymes involved in general carbohydrate metabolism. As for the CLR-1 experiments, we used ChIP-qPCR to validate the MC-CLR-2 ChIPseq experiments and confirmed enrichment of MC-CLR-2 at the promoter sites of the major cellulases encoded by *cbh-1*, *gh6-2*, and *gh6-3* (see Fig. S2). To identify the CLR-2 DNA binding motif, the 114 CLR-2 bound regions were inspected and the motif CGGN11CCG was identified in ~60% of the peaks (Fig. 3C; E value, $6.1E^{-20}$). The CLR-2 motif was found near the center of the ChIPseq binding regions. The CLR-2 DNA binding motif was nearly identical to that of the well-characterized *Saccharomyces cerevisiae* transcription factor Gal4p (*P* value, 7.6e-05) (Fig. 3C), which is the yeast homolog closest to *clr-2*.

By combining ChIPseq and RNAseq data (9) obtained from strains carrying the constitutively expressed *clr-2* allele, we identified 54 genes that were bound by CLR-2 and were dependent on

TABLE 2 Genes upregulated and differentially expressed in wild-type strain versus a *clr-2* constitutive expression strain and whose promoter region was bound by CLR-2

NCU no.	Locus	Annotation or domain
NCU00206[a]	*cdh-1*	Cellobiose dehydrogenase
NCU00762[a]	*gh5-1*	Glycosylhydrolase family 5
NCU00801[a]	*cdt-1*	Cellodextrin transporter
NCU00836[a]	*gh61-7*	Polysaccharide monooxygenase (AA9 family)
NCU00870		SET domain
NCU01049[c]		Fasciclin domain
NCU01050[a,c]	*gh61-4*	Polysaccharide monooxygenase (AA9 family)
NCU01076		Hypothetical protein
NCU01900[b]	*gh43-2*	Xylosidase/arabinosidase
NCU02009		Ferric reductase domain
NCU02059	*apr-3*	Endothiapepsin
NCU02138		Hypothetical protein
NCU02240[a]	*gh61-1*	Polysaccharide monooxygenase (AA9 family)
NCU02855	*gh11-1*	Endo-1,4 β-xylanase
NCU02915[a]		RhoGAP domain
NCU02916[a]	*gh61-3*	Polysaccharide monooxygenase (AA9 family)
NCU03180[c]		Hypothetical protein
NCU03181[c]		Acetylxylan esterase
NCU03328[c]	*gh61-6*	Polysaccharide monooxygenase (AA9 family)
NCU03329[c]		Domain of unknown function (DUF3632)
NCU04850	*gh55-1*	Exo-β-1,3-glucanase
NCU04854	*gh7-2*	Endoglucanase
NCU04870[b]	*ce1-1*	Acetyl xylan esterase
NCU05057[a]	*gh7-1*	Endoglucanase
NCU05121	*gh45-1*	Glycosylhydrolase family 45
NCU05846[a]		DUF1479
NCU05864[a]		Hypothetical protein
NCU05924	*gh10-1*	Endo-1,4-β-xylanase
NCU05955[a,c]	*gh74-1*	Cel74a; xyloglucanase
NCU05956[c]	*gh2-2*	β-Galactosidase
NCU06277		Microtubule-associated protein domain
NCU07143		6-Phosphogluconolactonase
NCU07190[a]	*gh6-3*	Exoglucanase 3
NCU07225[b]	*gh11-2*	Endo-1,4-β-xylanase
NCU07326	*gh32*	Glycosylhydrolase family 32
NCU07339[a,c]		Hypothetical protein
NCU07340[a,c]	*cbh-1*	Cellobiohydrolase
NCU07760	*gh61-2*	Polysaccharide monooxygenase (AA9 family)
NCU07787	*ccg-14*	Clock-controlled protein; cerato-platanin domain
NCU07897[a,c]		HET domain
NCU07898[a,c]	*gh61-13*	Polysaccharide monooxygenase (AA9 family)
NCU08114[b]	*cdt-2*	Cellodextrin transporter
NCU08397		Oligopeptide transporter domain
NCU08398		Aldose 1-epimerase
NCU08409	*trp-3*	Tryptophan synthetase
NCU08412[a]		Endo-β-1,4-mannanase
NCU08760	*gh61-5*	Polysaccharide monooxygenase (AA9 family)
NCU09416		Cellulose-binding GDSL lipase/acylhydrolase
NCU09523[a,c]		Hypothetical protein
NCU09524[a,c]		Cellulose binding domain
NCU09582	*ce4-1*	Chitin deacetylase
NCU09680[a]	*gh6-2*	Exoglucanase
NCU09764	*gh61-14*	Polysaccharide monooxygenase (AA9 family)
NCU09775	*gh54-1*	α-*N*-Arabinofuranosidase

[a] NCU numbers in bold indicate promoter regions of genes bound by both CLR-1 and CLR-2.

[b] NCU numbers in bold and in italics indicate promoter regions of genes bound by both CLR-2 and XLR-1.

[c] NCU numbers indicate promoter regions that may regulate 2 genes in opposite orientations.

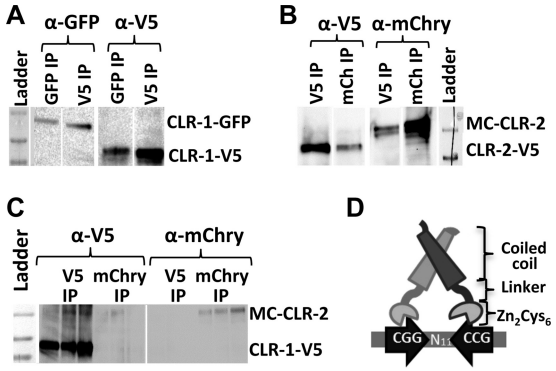

FIG 4 Coimmunoprecipitation experiments with CLR-1 and CLR-2. (A) Coimmunoprecipitation experiments were performed on a strain bearing CLR-1-GFP and CLR-1-V5. Data are from the same gel, differentially blotted with either α-GFP or α-V5 antibodies. Intervening control and blank lanes were removed. CLR-1-V5 is 81 kDa, and CLR-1-GFP is 105 kDa. Molecular mass markers (135 kDa, 95 kDa, and 72 kDa) are shown in the left lane. (B) Coimmunoprecipitation experiments were performed with a strain bearing MC-CLR-2 and CLR-2-V5. Data are from the same gel, differentially blotted with either α-V5 or α-mCherry (mChry) antibodies. Intervening control and blank lanes were moved. CLR-2-V5 is 93 kDa in size, while MC-CLR-2 is 117 kDa. Molecular mass markers (135 kDa and 95 kDa) are shown in the right lane. (C) Lack of detection of coimmunoprecipitation of CLR-1/CLR-2 heterocomplexes in a strain bearing CLR-1-V5 and MC-CLR-2. Data are from the same gel, differentially blotted with either α-V5 or α-mCherry antibodies. Molecular mass markers (135 kDa, 95 kDa, and 72 kDa) are shown in the left lane. The intervening lanes were removed. (D) Cartoon of CLR-2 binding as a homodimer to its predicted DNA binding motif.

CLR-2 for expression (Fig. 3B and Table 2). These included genes encoding 31 enzymes predicted to act on plant-derived polysaccharides, two cellodextrin transporter genes (*cdt-1* and *cdt-2* [21]), a predicted oligopeptide transporter gene (NCU08397), seven genes encoding proteins with biochemical domains, four genes encoding enzymes with uncharacterized roles in plant cell wall deconstruction, and nine genes that either encoded hypothetical proteins or contained a conserved domain of unknown biochemical function (DUF or HET).

CLR-1 and CLR-2 function as homodimers. Over half of the genes that both were dependent upon functional CLR-1 for expression and had promoters that were bound by CLR-1 were also regulated and bound by CLR-2 (Tables 1 and 2). Five of these genes encoded lytic polysaccharide monooxygenases (LPMOs; AA9 family) involved in the oxidative cleavage of cellulose (32–34). In addition, the promoter of a cellobiose dehydrogenase gene, *cdh-1*, which encodes an enzyme involved in pH-dependent electron transfer to LPMOs (33, 35), was also bound by both CLR-1 and CLR-2.

An inspection of the promoter regions of these 21 dually regulated genes showed that CLR-1 and CLR-2 bound in close proximity to each other. Dimerization of Zn_2C_6 transcription factors can occur via hydrophobic repeats that form a coiled-coil interaction region adjacent to the Zn_2C_6 domain (36). Analysis of CLR-1 and CLR-2 revealed a high probability of the presence of a coiled-coil structure in CLR-2 and, to a lesser extent, in CLR-1 (Fig. 4D; see also Fig. S3 in the supplemental material) (37). To test the hypothesis that CLR-1 and CLR-2 function either as homocomplexes or heterocomplexes, we first constructed strains that simultaneously expressed *clr-1-gfp* and *clr-1-V5* (see Text S1). As shown in Fig. 4A, CLR-1-V5 coimmunoprecipitated with CLR-1-GFP from Avicel-exposed mycelia, indicating that CLR-1 forms a homocomplex. To assess whether CLR-2 forms a homocomplex, we constructed a strain that carried a *clr-2* allele tagged with a V5 epitope at the *clr-2* locus and which showed WT endoglucanase levels (Fig. 1). Using a strain bearing both *mc-clr-2* and *clr-2-V5* strain constructs, MC-CLR-2 and CLR-2-V5 were coimmunoprecipitated, indicating that CLR-2 also forms a homocomplex (Fig. 4B). To test whether CLR-1 and CLR-2 function in a heterocomplex, a strain was constructed that expressed *clr-1-gfp* and also expressed *mc-clr-2* (see Text S1). However, although both CLR-1-GFP and MC-CLR-2 could be individually immunoprecipitated from the *clr-1-gfp*; *mc-clr-2* strain (Fig. 4C), coimmunoprecipitation of CLR-1-GFP with MC-CLR-2 was not detected, suggesting that CLR-1 and CLR-2 do not form a heterocomplex. To investigate this further, we sought to determine if the ability of constitutively expressed *mc* and *clr-2* genes to induce cellulase expression under sucrose conditions was dependent on the presence of CLR-1. To do this, we crossed the *mc-clr-2* strain with a *clr-1* deletion strain (Δ*clr-1*). The resulting p*ccg-1-mc-clr-2*; Δ*clr-1* strain was still capable of secreting cellulases even under sucrose conditions (Fig. 1B), supporting the notion that a CLR-1/CLR-2 heterocomplex is not a requirement for activation of cellulase gene transcription.

Construction of a *xlr-1* mutant that expresses hemicellulases under noninducing conditions. It was recently shown that a point mutation in *T. reesei xyr1* (Fig. 5A) rendered Xyr1 constitutively active (38) and that overexpression of wild-type *xyr1* was sufficient for activity under noninducing conditions (39). We therefore assessed whether constitutive expression of a strain with the wild-type *xlr-1* gene (p*ccg-1-xlr-1-gfp* strain) or a strain carrying the homologous *T. reesei* mutation (A828V) in *xlr-1* (p*ccg-1-xlr-1*^{A828V} strain) resulted in constitutive hemicellulase expression in *N. crassa*. Neither the wild-type strain nor the strain with constitutively expressed *xlr-1* secreted active xylanases under no-carbon conditions. However, a strain bearing the *xlr-1*^{A828V} mutation secreted active xylanases when switched to no-carbon media (Fig. 5B) and secreted significantly more active xylanase than either the WT or *xlr-1-gfp*-tagged strain when switched to xylan (Fig. 5C).

RNAseq analyses of the *xlr-1*^{A828V} mutant, the Δ*xlr-1* mutant, and the WT strain revealed the presence of both *xlr-1*-dependent and *xlr-1*-independent xylan-induced genes. As shown in Fig. 6A, the pattern of induction and expression of the dominant hemicellulase genes in the *xlr-1*^{A828V} mutant under no-carbon conditions was remarkably similar to that of a WT strain exposed to xylan (see Dataset S3 in the supplemental material). A cluster of 50 xylan-inducible genes were responsive to the *xlr-1*^{A828V} mutant and the WT strain under xylan conditions (Fig. 6B; cluster 1) and were dominated by xylanases and xylose-utilization genes. XLR-1-independent, xylan-induced genes in a second cluster (100 genes) were dominated by pectinases (Fig. 6B; cluster 2). These genes were induced in strains switched to pectin media (7), suggesting that this large cluster of genes is induced by pectin contamination of the xylan substrate and not by xylan *per se*.

XLR-1 target gene regulon. To identify direct targets of XLR-1, we used a p*ccg-1-xlr-1-gfp*; Δ*xlr-1* strain, which showed endoxylanase activity and secreted protein levels comparable to those seen with the WT strain (Fig. 5C). Under xylan conditions, XLR-1-GFP bound to 63 sites, corresponding to promoters for 84 genes (see Dataset S1 in the supplemental material), including

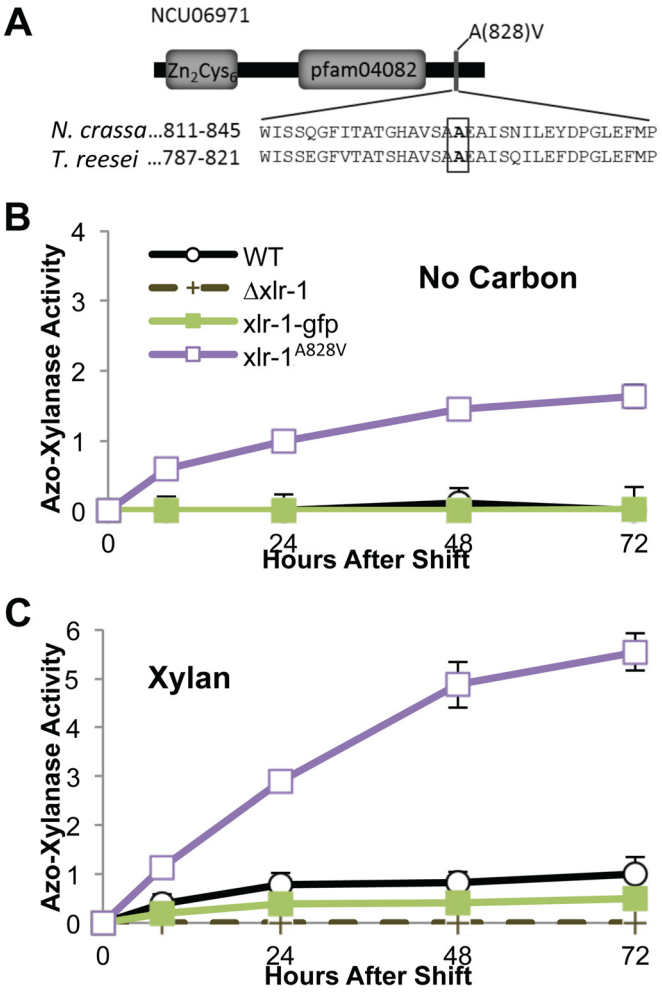

FIG 5 A *xlr-1*^{A828V} strain shows constitutively active hemicellulose activity under noninducing conditions. (A) Cartoon of *N. crassa* XLR-1 showing the alanine-to-valine mutation and alignment to the corresponding region of a constitutively activating mutation in *T. reesei* Xyr1 (38). (B) Endoxylanase activity of the strain bearing the *xlr-1*^{A828V} allele under noninducing (no-carbon) conditions relative to the parental wild type, a strain carrying p*ccg-1*-driven *xlr-1-gfp*, and the Δ*xlr-1* deletion strain. (C) Endoxylanase activity of strains shown in panel B with xylan as the sole carbon source. Endoxylanase activity in panels B and C was normalized to wild-type xylan cultures from panel C.

genes for 6 hemicellulases (*gh10-2*, *gh11-1*, *gh11-2*, *gh115-1*, *gh43-2*, and *gh51-1*); 3 acetylxylan esterases (*ce1-1*, *ce1-4*, and *ce5-2*); a β-glucosidase (*gh1-1*); two β-xylosidases (*gh43-5* and *gh3-8*), and key enzymes in xylose utilization (*xyr-1*, *xdh*, *xk*, and the gene encoding ribose 5-phosphate isomerase [NCU10107]). In addition, genes encoding five predicted transporters (including *cdt-2* and the gene for a xylose transporter [NCU06138]) and two transcription factors (*clr-1* and *vib-1*) were bound by XLR-1. The 84 regions bound by XLR-1 showed enrichment for the motif GGN TAAA (*E* value, 1.2E^{-36}) (Fig. 6D), which matched an XlnR consensus motif proposed for three *Aspergillus* species (40).

Deletion mutants of *xlr-1* slightly affect cellulase activity (8), and *xlr-1* homologs in other fungi regulate both cellulase and hemicellulase genes (11, 12, 41–43). We therefore performed ChIPseq on the *xlr-1 gfp* strain after a switch to Avicel medium (see Dataset S1 in the supplemental material). The XLR-1-bound promoter regions were similar under xylan and Avicel conditions, with an overlap of 94%. However, enrichment of XLR-1 binding sites on the promoters of major hemicellulase genes was an order of magnitude lower under Avicel conditions than under xylan conditions (see Fig. S2B in the supplemental material), reflective of weak activation of XLR-1 by trace xylan contamination of Avicel (19). Importantly, the promoters of genes encoding cellulases were not bound by XLR-1 under any of the tested conditions.

Directly bound targets of XLR-1 that were also dependent on XLR-1 for expression in the *xlr-1*^{A828V} mutant revealed a set of 23 genes (Fig. 6C and Table 3; see also Dataset S2 in the supplemental material). This gene set was dominated by genes encoding secreted enzymes required for deconstruction of xylan and by genes encoding enzymes involved in xylobiose or xylose utilization and a xylose/glucose transporter. In addition, other uncharacterized sugar transporters (NCU04537 and NCU05350) and two hypothetical proteins (NCU06490 and NCU07510) were in this gene set (Table 3).

Network analysis of lignocellose deconstruction. The plant cell wall is a multivariate structure that requires the orchestrated and concerted action of enzymes involved in cellulose, hemicellulose, pectin, and lignin activity for deconstruction. Four target genes were directly bound by both CLR-2 and XLR-1 and were also differentially expressed in the *clr-2* and *xlr-1* mutant strains versus the WT strain. These genes included *gh43-2* (encoding xylosidase/arabinosidase), *cel-1* (acetyl xylan esterase), *gh11-2* (endoxylanase), and *cdt-2* (cellodextrin transporter), which are predicted to be involved in xylan degradation, including the CDT-2 transporter (44). Two of these targets, *cdt-2* and *gh11-2*, were also bound by CLR-1 (see Dataset S1 in the supplemental material), suggesting a direct role for all three transcription factors in their regulation. By combining genome-wide expression studies using RNAseq and direct binding studies using ChIPseq to identify the direct-target regulons for CLR-1, CLR-2, and XLR-1, we resolved many of the issues associated with translating raw ChIPseq data into meaningful assignment of biological function. Network analyses showed that CLR-1, CLR-2, and XLR-1 bind the promoters of and regulate the expression of genes encoding cellulases and hemicellulases and also of genes encoding a wide array of other transcription factors and transporters and of genes involved in carbohydrate metabolism as well as genes of unknown biochemical function (Fig. 7; the xylan network is shown in Fig. S4 in the supplemental material). Within this network, the CLR-1, CLR-2, and XLR-1 regulons are clearly distinct but overlap in many of the most highly and differentially expressed genes, underscoring the importance of regulation of these target genes on multiple levels and the regulatory effects of having multiple bound transcription factors for plant cell wall deconstruction.

DISCUSSION

The regulatory network coordinating plant cell wall hydrolysis and utilization reflects the complex and variable nature of plant cell wall polysaccharides. Some dedicated enzymes (such as cellulases and hemicellulases) need to be regulated independently of enzymes specific for other polymers (pectin, for example), while some genes with broader functionality (such as those encoding general oligosaccharide transporters) must be additively regulated in response to multiple signals. Concurrently with the restructuring of the transcriptional landscape, the metabolic stress of shift-

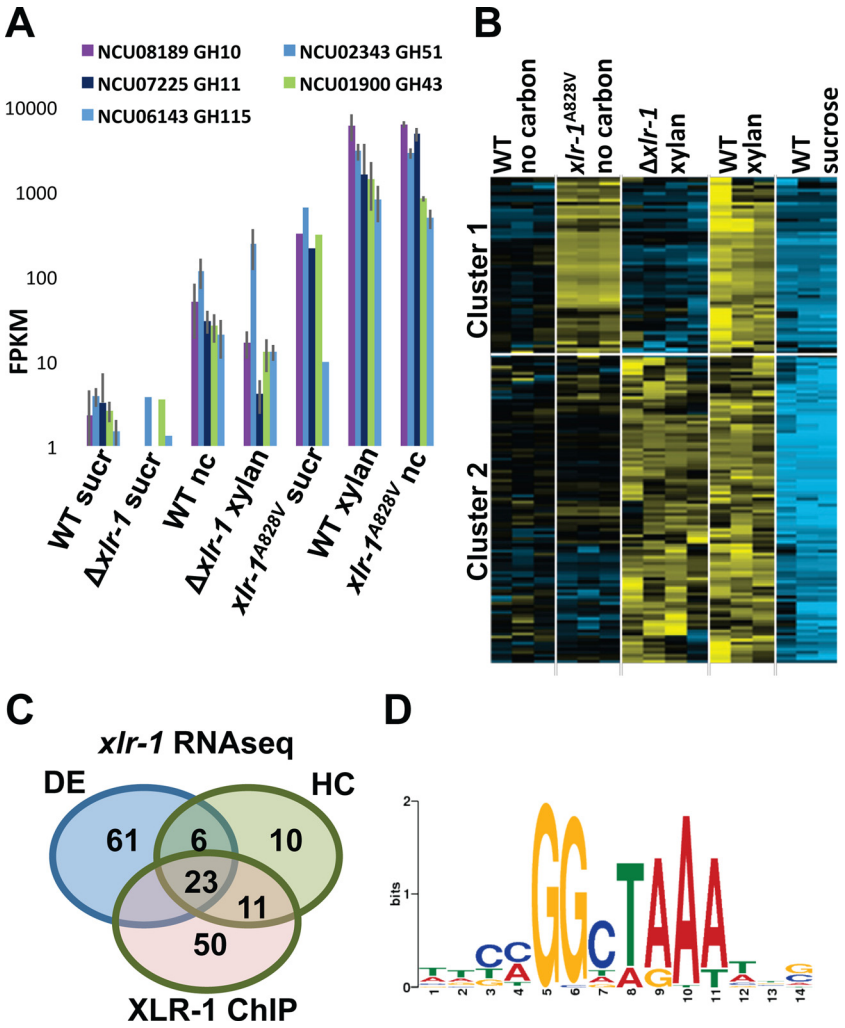

FIG 6 Identification of XLR-1 regulon, direct targets, and XLR-1 binding site. (A) RNAseq analyses of the most highly expressed hemicellulase genes in the *xlr-1*^{A828V} strain relative to the WT strain and a Δ*xlr-1* mutant shifted to sucrose (sucr), no-carbon (nc), or xylan medium conditions. (B) Hierarchical clustering of gene expression of the strains shown shifted to sucrose, no-carbon, or xylan conditions. Genes within cluster 1 are dependent upon XLR-1 for expression. (C) Venn diagram depicting overlap of genes that show differential expression (DE), genes that have similar expression patterns through hierarchical clustering (HC) in the WT strain versus the *xlr-1*^{A828V} strain under no-carbon conditions (Cuffdiff; Padj = <0.05; 4-fold), and genes that showed significant binding of XLR-1 in their promoter regions (XLR-1 ChIP). (D) Consensus binding sequence for XLR-1 based on promoter regions bound by XLR-1 in the ChIPseq data.

ing global protein expression to largely secreted proteins requires fine-tuning of many aspects of intracellular carbon metabolism, secretion, and even cellular morphology. In *N. crassa*, CLR-1, CLR-2, and XLR-1 form the nexus of this complex regulatory lignocellulosic deconstruction network.

This report presents genome-wide analyses of the three major transcription factors required for deconstruction of the major components of the plant cell wall. A total of 39 and 54 genes in a core set are directly bound and regulated by CLR-1 and CLR-2, respectively, under cellulosic conditions, and 23 genes are bound and regulated by XLR-1 under xylan conditions. The CLR-1, CLR-2, and XLR-1 regulons were distinct but overlapped in some of the most highly and differentially expressed genes. A prime example is the gene encoding cellodextrin transporter 2, *cdt-2*, which is bound and differentially expressed and contains the XLR-1 and CLR-2 motifs and a partial CLR-1 motif (CGGNC CG). Regulation by all three transcription factors is consistent with recent findings indicating that *cdt-2* encodes a generalized oligosaccharide transporter capable of transporting both cellodextrins and xylodextrins (44, 45). CLR-1, CLR-2, and XLR-1 also each bound to genes encoding additional transcription factors, including ones that have a role in regulating nutrient sensing under cellulolytic conditions in *N. crassa*, such as *vib-1* (24), *cpc-1* (*cross-pathway-control-1*) (25), *sah-2* (29), and *hac-1*, which regulates the unfolded protein response and was recently shown to be required for cellulose utilization (30, 31). These transcription factors could act as drivers for second-tier gene expression, allowing more-nuanced regulation in response to different carbon sources.

Previously, *clr-1* was identified as a target of the white-collar complex (WCC) composed of WC-1 and WC-2 (46), which is the major blue light and clock regulator in *N. crassa* (47, 48). Light affects expression of cellulases in both *N. crassa* and *T. reesei* (25, 49). During light and circadian regulation, WCC activates the major circadian regulator, *frq*, which functions as a negative regulatory element in the circadian negative-feedback loop (48, 50). We found that CLR-1 bound the promoter region of *frq* under sucrose

TABLE 3 Genes upregulated and differentially expressed in the wild-type strains versus a *xlr-1*^{A828V} constitutive expression strain and whose promoter regions was bound by XLR-1

NCU no.	Locus	Annotation or domain
NCU00292	*cea-3*	Carboxy esterase
NCU00709	*gh3-8*	β-Xylosidase
NCU00891	*Xdh*	Xylitol dehydrogenase
NCU01900[a]	*gh43-2*	Xylosidase/arabinosidase
NCU02343	*gh51-1*	Alpha-L-arabinofuranosidase
NCU03322		GDSL family lipase
NCU04401		Fructose-bisphosphate aldolase
NCU04537		Monosaccharide transporter
NCU04870[a]	*ce1-1*	Acetyl xylan esterase
NCU05159	*ce5-2*	Acetyl xylan esterase
NCU05350		Major facilitator transporter
NCU06138	*xy-31*	Xylose transporter
NCU06143	*gh115-1*	Putative glucuronidase
NCU06490		Hypothetical protein
NCU07225[a]	*gh11-2*	Endo-1,4-β-xylanase
NCU07510		Hypothetical protein
NCU08114[a]	*cdt-2*	Cellodextrin/xylodextrin transporter
NCU08189	*gh10-2*	Endo-1,4-β-xylanase
NCU08384	*xyr-1*	Xylose reductase
NCU09652	*gh43-5*	β-Cylosidase
NCU09705		GAL10-like; UDP-glucose-4-epimerase
NCU10110		3-Hydroxyisobutyrate dehydrogenase
NCU11353	*xyk-1*	D-Xylulose kinase

[a] NCU numbers in bold indicate promoter regions bound by CLR-2 and XLR-1.

and Avicel conditions. The conditions under which our experiments were performed for ChIPseq and RNAseq analyses reduced or eliminated the light and clock inputs. However, the binding of the *clr-1* promoter by the WCC and binding of the promoter of *frq* by CLR-1 suggest interplay among light, clock regulation, and plant cell wall deconstruction in filamentous fungi, which deserves further investigation.

Promoter regions of genes directly bound by CLR-1, CLR-2, and XLR-1 included genes encoding a number of hypothetical proteins or proteins that have predicted functional domains but that do not have a characterized connection to plant biomass deconstruction or utilization. In particular, constitutive expression of CLR-2 and XLR-1^{A828V} resulted in secretion of cellulase and hemicellulases, respectively, under noninducing conditions. The CLR-1/CLR-2 and XLR-1 regulons, as determined on the basis of RNAseq data, are large (212 and 243 genes, respectively); approximately 50% of the genes in each of these regulons encode hypothetical proteins or proteins with a generalized biochemical function, thus making establishing priorities for biochemical characterization difficult. Identifying the genes that are directly regulated by CLR-1, CLR-2, and XLR-1 considerably reduced this list of genes. For example, two hypothetical proteins (encoded by NCU06490 and NCU07510) and two uncharacterized transporters (encoded by NCU05350 and NCU04537) are bound by XLR-1, suggesting that these proteins play a role in xylan degradation/utilization and sugar transport, respectively. Similarly, 20 genes in the CLR-2 direct regulon (Table 2) encode proteins that do not have an obvious role in deconstruction of plant biomass.

Although CLR-1 bound to two-thirds of its regulon under sucrose conditions, the promoters of many cellulase genes were not bound; unlike the results seen with *clr-2*, constitutive expression of *clr-1* did not result in significant cellulase activity. These data indicate that CLR-1 requires an activating step, presumably via cellulose sensing. In addition, carbon catabolite repression (CCR) functions to repress expression of cellulolytic genes under noninducing conditions (51). It is possible that CLR-1 (and its targets) is also subject to regulation by CCR, which may affect its activity and ability to bind target genes, with binding to some targets more strongly affected than binding to others.

By leveraging the ChIPseq data, we identified DNA binding motifs for CLR-1, CLR-2, and XLR-1. In a recent study, the binding sites of over 1,000 transcription factors were determined *in vitro* by protein binding microarrays (PBM) (52); XLR-1 and CLR-1 were included in that analysis. The PBM analyses identified only the conserved "A" residue as significant; however, the overall sequence, including nucleotides below the confidence threshold, matches the XLR-1 motif identified here. For the CLR-1 motif, the PBM analyses identified the CGG triplet common to all Zn_2C_6 transcription factors (52). The CLR-2 binding site was not identified via PBM analyses (52), but here we show that the *clr-2* DNA binding motif is identical to that of *S. cerevisiae* Gal4p, which is the closest paralog to CLR-2 in the *N. crassa* genome, consistent with the finding that proteins with conserved DNA binding domains bind highly similar DNA sequences (52). CLR-2 does not target galactose utilization genes, highlighting the conserved nature of these transcription factors even as their target genes have diverged over time. In addition, the regulation of CLR-2 is clearly different from the posttranslational regulation of Gal4p (53). By directly assaying their DNA binding locations *in vivo* on model plant cell wall substrates and tying that binding to functional induction of target genes, we have reaffirmed several known components of that network and highlighted new points of coordination among

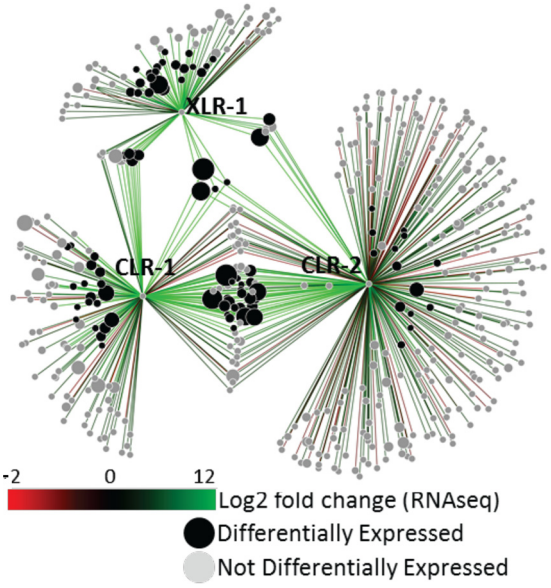

FIG 7 *N. crassa* regulatory network on Avicel. Edge-weighted, spring-embedded network model of ChIP-bound genes using fold change data from gene expression as the variable. The edges connecting nodes are colored according to a color gradient: red for downregulated genes, green for upregulated genes, and black for no change. Gray nodes represent genes that are not differentially expressed, and black nodes represent genes that are differentially expressed in RNAseq library comparisons of WT data determined under conditions of exposure to the negative control (NC) for 4 h versus WT data determined under conditions of exposure to Avicel for 4 h. Node sizes correspond to gene expression levels.

polymer saccharification, sugar transport, carbon metabolism, nutrient sensing, and cellular physiology. To engineer the next generation of hypersecreting industrial strains, all of these aspects will need to be explored and manipulated.

MATERIALS AND METHODS

Strains and growth conditions. The wild-type strain (FGSC 2489) and gene deletion mutants were obtained from the Fungal Genetics Stock Center (FGSC) (54, 55). A detailed list of the constructed *his-3*::p*ccg-1-mc-clr-2*; Δ*clr-2*::Hyg^r; *sad-1*::Hyg^r; *rid-1 A*, the *his-3*::p*ccg-1-xlr-1*^{A828V}; Δ*xlr-1*::Hyg^r *a*, the *clr-1-V5*::Hyg^r *a*, the *clr-2-V5*::Hyg^r *a*, *his-3*::p*ccg-1-xlr-1-gfp*; Δ*xlr-1*::Hyg^r, and the *his-3*::p*ccg-1-clr-1-gfp*; Δ*clr-1*::Hyg^r *A* strains is provided in Text S1 in the supplemental material. All strains were propagated on 2% sucrose Vogel's minimal medium (VMM) slants, grown in the dark at 30C for 2 days, and transferred to conditions of constant light at 25°C for all downstream experiments.

Enzyme and secreted protein assays. CMCase and xylanase activity assays were carried out according to the protocols of the manufacturer (Megazyme) (S-ACMCL and S-AXBL), with slight modifications. Reaction mixtures were miniaturized to 200 μl in 100 mM sodium acetate (pH 5.0), and a lower substrate concentration (0.3%) was used with 5 to 20 μl of culture supernatants. After incubation at 50°C for 30 min, uncleaved polymers were precipitated with 1 ml of ethanol and relative enzyme activities measured by absorbance of the supernatant at 590 nm. Total protein was determined by Bradford assays (BioRad).

Chromatin immunoprecipitation. Flasks containing 100 ml VMM–2% (wt/vol) sucrose were inoculated with 10^6 conidia and incubated 16 h at 25°C under conditions of constant light at 220 rpm. The experimental conditions for the ChIPseq data are provided in Table S1 in the supplemental material. The culture was filtered, rinsed with Dulbecco's phosphate-buffered saline (DPBS; Invitrogen), and transferred to 100 ml fresh VMM containing 1% cellulose (Avicel PH-101; Sigma-Aldrich), hemicellulose (Beechwood xylan; Sigma-Aldrich), or sucrose as the sole carbon source for 4 h (3 biological replicates each for the *clr-1-gfp*, *mc-clr-2*, and *xlr-1-gfp* strains on Avicel, 3 biological replicates for the *xlr-1-gfp* strain on xylan, and 1 biological replicate for the *clr-1-V5* strain on Avicel). In addition, *N. crassa clr-1-gfp*, *mc-clr-2*, p*ccg-1-gfp*, and p*ccg-1-mCherry* strains were grown for 16 h on sucrose and switched to Avicel for 24 h prior to fixation. Cells were fixated in 1% formaldehyde. After 15 min, the reaction was quenched by a 5-min incubation in 125 mM glycine. Cells were harvested by filtration, flash frozen in liquid nitrogen, and stored at −80°C. Chromatin immunoprecipitation was carried out using versions of previously published protocols (46) (briefly described in Text S1). ChIPseq files are available at the NCBI GEO database (accession no. GSE68517).

ChIPseq peak calling and motif analyses. Enriched peaks were identified with MACS (v1.4.2) (56) (see Dataset S1 in the supplemental material). Peaks that overlapped by 50% across replicates were identified with Bedtools (v2.16.2) (57). Peaks were manually curated to remove false positives. Surrounding genes were extracted with a custom Perl script. This list was manually curated to remove genes with no detectable transcription. A total of 300 bp of sequence data from either side of each summit were analyzed for enriched motifs with the MEME-ChIP suite (v4.9.1): a compilation of MEME, DREME, CentriMo, and TomTom (58) (http://meme.nbcr.net/meme/).

Differential-expression analysis. RNAseq libraries included WT (FGSC 2489) and Δ*xlr-1* strains grown for 16 h in VMM and switched to xylan (Beechwood xylan; Sigma-Aldrich) for 4 h (3 biological replicates) and the *xlr-1*^{A828V} strain grown for 16 h in VMM and transferred to either sucrose or media containing no carbon source for 4 h (3 biological replicates). RNA libraries were generated following the Illumina protocols and sequenced on the Illumina HiSeq 2000 platforms. The expression sequence files are available at the NCBI GEO database (accession no. GSE68517). Mapping and analyses were as previously described (9) (see Text S1 in the supplemental material).

Hierarchical clustering analysis was performed with the Cluster 3.0/TreeView software suite (http://bonsai.hgc.jp/~mdehoon/software/cluster/software.htm). Fragments per kilobase per million (FPKMs) were normalized with the average linkage method with Pearson's uncentered correlation as the similarity metric. Network analysis was performed using cytoscape 3.1.1 (59).

Coimmunoprecipitation experiments. Strains were grown for 16 h on VMM and subsequently switched to Avicel for 4 h. One gram of mycelia was ground and suspended in 2 ml DPBS buffer with protease inhibitors (0.1 M phenylmethylsulfonyl fluoride [PMSF], Complete EDTA-free protease inhibitors). The suspension was processed with a Dounce homogenizer 10 times and cross-linked with 3 mM dithiobis succinimidyl propionate (DSP) for 2 h. The reaction was quenched with 1 M Tris (pH 7.5) to reach a final concentration of 25 mM Tris for 15 min at room temperature. Final concentrations of 1% NP-40 and 0.5% deoxycholate were added to disrupt nuclear membranes. Immunoprecipitation was carried out as described above for ChIP (mouse anti-GFP [Roche; 11814460001], rabbit anti-mCherry [BioVision; 5993-100], and rabbit anti-V5 [Abcam; ab9116]). Western blot analyses were performed as previously described (see Text S1 in the supplemental material).

ChIP-qPCR analysis. A CFX Connect real-time PCR machine (Bio-Rad) and DyNAmo HS Sybr green master mix (Thermo Scientific) were used for qPCR experiments. All primers (see Text S1 in the supplemental material) were assessed for amplification efficiency using a serial dilution of genomic DNA (data not shown). Negative controls (NC-1, NC-2, NC-3, and NC-4) were composed of regions devoid of nearby genes, and primers for the promoter region of GAPDH (glyceraldehyde-3-phosphate dehydrogenase) (NCU01528) were designed for use as the nontarget control. qPCR was carried out with chromatin-immunoprecipitated DNA, and fold enrichment was determined by comparing the antibody immunoprecipitated fraction to a no-antibody precipitated control.

SUPPLEMENTAL MATERIAL

Supplemental material for this article may be found at http://mbio.asm.org/lookup/suppl/doi:10.1128/mBio.01452-15/-/DCSupplemental.

Text S1, PDF file, 0.1 MB.
Dataset S1, XLSX file, 0.2 MB.
Dataset S2, XLSX file, 0.1 MB.
Dataset S3, XLSX file, 1.3 MB.
Figure S1, PDF file, 0.2 MB.
Figure S2, PDF file, 0.4 MB.
Figure S3, PDF file, 0.1 MB.
Figure S4, PDF file, 1 MB.
Table S1, PDF file, 0.1 MB.

ACKNOWLEDGMENTS

This work was supported by a grant from Energy Biosciences Institute to N.L.G. and National Institutes of Health NRSA Trainee Grant 2 T32 GM 7127-36 A1 to S.T.C.

J.P.C. performed the ChIP work, motif analysis, Co-IP work, and RNAseq analysis and drafted the manuscript. S.T.C. performed the *xlr-1* mutation analysis, RNAseq library construction, and enzyme assays and aided in drafting the manuscript. T.L.S. created vector pTS12 and edited the manuscript. N.L.G. was involved in the study's conception and design and in preparation and editing of the manuscript.

REFERENCES

1. **Carroll A, Somerville C.** 2009. Cellulosic biofuels. Annu Rev Plant Biol **60:**165–182. http://dx.doi.org/10.1146/annurev.arplant.043008.092125.
2. **Klein-Marcuschamer D, Oleskowicz-Popiel P, Simmons BA, Blanch HW.** 2012. The challenge of enzyme cost in the production of lignocellulosic biofuels. Biotechnol Bioeng **109:**1083–1087. http://dx.doi.org/10.1002/bit.24370.
3. **MacLean HL, Spatari S.** 2009. The contribution of enzymes and process chemicals to the life cycle of ethanol. Environ Res Lett **4:**014001. http://dx.doi.org/10.1088/1748-9326/4/1/014001.
4. **Turner BC, Perkins DD, Fairfield A.** 2001. *Neurospora* from natural

populations: a global study. Fungal Genet Biol **32:**67–92. http://dx.doi.org/10.1006/fgbi.2001.1247.

5. **Jacobson DJ, Dettman JR, Adams RI, Boesl C, Sultana S, Roenneberg T, Merrow M, Duarte M, Marques I, Ushakova A, Carneiro P, Videira A, Navarro-Sampedro L, Olmedo M, Corrochano LM, Taylor JW.** 2006. New findings of *Neurospora* in Europe and comparisons of diversity in temperate climates on continental scales. Mycologia **98:**550–559. http://dx.doi.org/10.3852/mycologia.98.4.550.
6. **Coradetti ST, Craig JP, Xiong Y, Shock T, Tian C, Glass NL.** 2012. Conserved and essential transcription factors for cellulase gene expression in ascomycete fungi. Proc Natl Acad Sci U S A **109:**7397–7402. http://dx.doi.org/10.1073/pnas.1200785109.
7. **Benz JP, Chau BH, Zheng D, Bauer S, Glass NL, Somerville CR.** 2014. A comparative systems analysis of polysaccharide-elicited responses in *Neurospora crassa* reveals carbon source-specific cellular adaptations. Mol Microbiol **91:**275–299. http://dx.doi.org/10.1111/mmi.12459.
8. **Sun J, Tian C, Diamond S, Glass NL.** 2012. Deciphering transcriptional regulatory mechanisms associated with hemicellulose degradation in *Neurospora crassa*. Eukaryot Cell **11:**482–493. http://dx.doi.org/10.1128/EC.05327-11.
9. **Coradetti ST, Xiong Y, Glass NL.** 2013. Analysis of a conserved cellulase transcriptional regulator reveals inducer-independent production of cellulolytic enzymes in *Neurospora crassa*. Microbiologyopen **2:**595–609. http://dx.doi.org/10.1002/mbo3.94.
10. **Calero-Nieto F, Di Pietro A, Roncero MIG, Hera C.** 2007. Role of the transcriptional activator *xlnR* of *Fusarium oxysporum* in regulation of xylanase genes and virulence. Mol Plant Microbe Interact **20:**977–985. http://dx.doi.org/10.1094/MPMI-20-8-0977.
11. **Van Peij NN, Gielkens MM, de Vries RP, Visser J, de Graaff LH.** 1998. The transcriptional activator XlnR regulates both xylanolytic and endoglucanase gene expression in *Aspergillus niger*. Appl Environ Microbiol **64:**3615–3619.
12. **Marui J, Kitamoto N, Kato M, Kobayashi T, Tsukagoshi N.** 2002. Transcriptional activator, AoXlnR, mediates cellulose-inductive expression of the xylanolytic and cellulolytic genes in *Aspergillus oryzae*. FEBS Lett **528:**279–282. http://dx.doi.org/10.1016/S0014-5793(02)03328-8.
13. **Yao G, Li Z, Gao L, Wu R, Kan Q, Liu G, Qu Y.** 2015. Redesigning the regulatory pathway to enhance cellulase production in *Penicillium oxalicum*. Biotechnol Biofuels **8:**71. http://dx.doi.org/10.1186/s13068-015-0253-8.
14. **Stricker AR, Grosstessner-Hain K, Wurleitner E, Mach RL.** 2006. Xyr1 (xylanase Regulator 1) regulates both the hydrolytic enzyme system and D-xylose metabolism in *Hypocrea jecorina*. Eukaryot Cell **5:**2128–2137. http://dx.doi.org/10.1128/EC.00211-06.
15. **Brunner K, Lichtenauer AM, Kratochwill K, Delic M, Mach RL.** 2007. Xyr1 regulates xylanase but not cellulase formation in the head blight fungus *Fusarium graminearum*. Curr Genet **52:**213–220. http://dx.doi.org/10.1007/s00294-007-0154-x.
16. **Klaubauf S, Narang HM, Post H, Zhou M, Brunner K, Mach-Aigner AR, Mach RL, Heck AJR, Altelaar AFM, de Vries RP.** 2014. Similar is not the same: differences in the function of the (hemi-)cellulolytic regulator XlnR (Xlr1/Xyr1) in filamentous fungi. Fungal Genet Biol **72:**73–81. http://dx.doi.org/10.1016/j.fgb.2014.07.007.
17. **Häkkinen M, Valkonen MJ, Westerholm-Parvinen A, Aro N, Arvas M, Vitikainen M, Penttilä M, Saloheimo M, Pakula TM.** 2014. Screening of candidate regulators for cellulase and hemicellulase production in *Trichoderma reesei* and identification of a factor essential for cellulase production. Biotechnol Biofuels **7:**14. http://dx.doi.org/10.1186/1754-6834-7-14.
18. **Sun J, Phillips CM, Anderson CT, Beeson WT, Marletta MA, Glass NL.** 2011. Expression and characterization of the *Neurospora crassa* endoglucanase GH5-1. Protein Expr Purif **75:**147–154. http://dx.doi.org/10.1016/j.pep.2010.08.016.
19. **Znameroski EA, Coradetti ST, Roche CM, Tsai JC, Iavarone AT, Cate JHD, Glass NL.** 2012. Induction of lignocellulose-degrading enzymes in *Neurospora crassa* by cellodextrins. Proc Natl Acad Sci U S A **109:**6012–6017. http://dx.doi.org/10.1073/pnas.1118440109.
20. **Phillips CM, Iavarone AT, Marletta MA.** 2011. Quantitative proteomic approach for cellulose degradation by *Neurospora crassa*. J Proteome Res **10:**4177–4185. http://dx.doi.org/10.1021/pr200329b.
21. **Galazka JM, Tian C, Beeson WT, Martinez B, Glass NL, Cate JHD.** 2010. Cellodextrin transport in yeast for improved biofuel production. Science **330:**84–86. http://dx.doi.org/10.1126/science.1192838.
22. **Xiong Y, Coradetti ST, Li X, Gritsenko MA, Clauss T, Petyuk V, Camp D, Smith R, Cate JHD, Yang F, Glass NL.** 2014. The proteome and phosphoproteome of *Neurospora crassa* in response to cellulose, sucrose and carbon starvation. Fungal Genet Biol **72:**21–33. http://dx.doi.org/10.1016/j.fgb.2014.05.005.
23. **Cai P, Wang B, Ji J, Jiang Y, Wan L, Tian C, Ma Y.** 2015. The putative cellodextrin transporter-like protein CLP1 is involved in cellulase induction in *Neurospora crassa*. J Biol Chem **290:**788–796. http://dx.doi.org/10.1074/jbc.M114.609875.
24. **Xiong Y, Sun J, Glass NL.** 2014. VIB1, a link between glucose signaling and carbon catabolite repression, is essential for plant cell wall degradation in *Neurospora crassa*. PLoS Genet **10:**e1004500. http://dx.doi.org/10.1371/journal.pgen.1004500.
25. **Schmoll M, Tian C, Sun J, Tisch D, Glass NL.** 2012. Unravelling the molecular basis for light modulated cellulase gene expression—the role of photoreceptors in *Neurospora crassa*. BMC Genomics **13:**127. http://dx.doi.org/10.1186/1471-2164-13-127.
26. **Tian C, Kasuga T, Sachs MS, Glass NL.** 2007. Transcriptional profiling of cross pathway control in *Neurospora crassa* and comparative analysis of the Gcn4 and CPC1 regulons. Eukaryot Cell **6:**1018–1029. http://dx.doi.org/10.1128/EC.00078-07.
27. **Paluh JL, Orbach MJ, Legerton TL, Yanofsky C.** 1988. The cross-pathway control gene of *Neurospora crassa*, *cpc-1*, encodes a protein similar to GCN4 of yeast and the DNA-binding domain of the oncogene v-jun-encoded protein. Proc Natl Acad Sci U S A **85:**3728–3732. http://dx.doi.org/10.1073/pnas.85.11.3728.
28. **Small AJ, Hynes MJ, Davis MA.** 1999. The TamA protein fused to a DNA-binding domain can recruit AreA, the major nitrogen regulatory protein, to activate gene expression in *Aspergillus nidulans*. Genetics **153:**95–105.
29. **Reilly MC, Qin L, Craig JP, Starr TL, Glass NL.** 2015. Deletion of homologs of the SREBP pathway results in hyper-production of cellulases in *Neurospora crassa* and *Trichoderma reesei*. Biotechnol Biofuels **8:**121. http://dx.doi.org/10.1186/s13068-015-0297-9.
30. **Montenegro-Montero A, Goity A, Larrondo LF.** 2015. The bZIP transcription factor HAC-1 is involved in the unfolded protein response and is necessary for growth on cellulose in *Neurospora crassa*. PLoS One **10:**e0131415. http://dx.doi.org/10.1371/journal.pone.0131415.
31. **Fan F, Ma G, Li J, Liu Q, Benz JP, Tian C, Ma Y.** 2015. Genome-wide analysis of the endoplasmic reticulum stress response during lignocellulase production in *Neurospora crassa*. Biotechnol Biofuels **8:**66. http://dx.doi.org/10.1186/s13068-015-0248-5.
32. **Beeson WT, Phillips CM, Cate JHD, Marletta MA.** 2012. Oxidative cleavage of cellulose by fungal copper-dependent polysaccharide monooxygenases. J Am Chem Soc **134:**890–892. http://dx.doi.org/10.1021/ja210657t.
33. **Phillips CM, Beeson WT, Cate JH, Marletta MA.** 2011. Cellobiose dehydrogenase and a copper-dependent polysaccharide monooxygenase potentiate cellulose degradation by *Neurospora crassa*. ACS Chem Biol **6:**1399–1406. http://dx.doi.org/10.1021/cb200351y.
34. **Quinlan RJ, Sweeney MD, Lo Leggio L, Otten H, Poulsen JN, Johansen KS, Krogh KBRM, Jorgensen CI, Tovborg M, Anthonsen A, Tryfona T, Walter CP, Dupree P, Xu F, Davies GJ, Walton PH.** 2011. Insights into the oxidative degradation of cellulose by a copper metalloenzyme that exploits biomass components. Proc Natl Acad Sci U S A **108:**15079–15084. http://dx.doi.org/10.1073/pnas.1105776108.
35. **Sygmund C, Kracher D, Scheiblbrandner S, Zahma K, Felice AKG, Harreither W, Kittl R, Ludwig R.** 2012. Characterization of the two *Neurospora crassa* cellobiose dehydrogenases and their connection to oxidative cellulose degradation. Appl Environ Microbiol **78:**6161–6171. http://dx.doi.org/10.1128/AEM.01503-12.
36. **Marmorstein R, Carey M, Ptashne M, Harrison SC.** 1992. DNA recognition by GAL4: structure of a protein-DNA complex. Nature **356:**408–414. http://dx.doi.org/10.1038/356408a0.
37. **Lupas A, Van Dyke M, Stock J.** 1991. Predicting coiled coils from protein sequences. Science **252:**1162–1164. http://dx.doi.org/10.1126/science.252.5009.1162.
38. **Derntl C, Gudynaite-Savitch L, Calixte S, White T, Mach RL, Mach-Aigner AR.** 2013. Mutation of the xylanase regulator 1 causes a glucose blind hydrolase expressing phenotype in industrially used *Trichoderma* strains. Biotechnol Biofuels **6:**62. http://dx.doi.org/10.1186/1754-6834-6-62.
39. **Lv X, Zheng F, Li C, Zhang W, Chen G, Liu W.** 2015. Characterization of a copper responsive promoter and its mediated overexpression of the xylanase regulator 1 results in an induction-independent production of

cellulases in *Trichoderma reesei*. Biotechnol Biofuels **8:**67. http://dx.doi.org/10.1186/s13068-015-0249-4.

40. **Andersen MR, Vongsangnak W, Panagiotou G, Salazar MP, Lehmann L, Nielsen J.** 2008. A trispecies *Aspergillus* microarray: comparative transcriptomics of three Aspergillus species. Proc Natl Acad Sci U S A **105:** 4387–4392. http://dx.doi.org/10.1073/pnas.0709964105.
41. **Stricker AR, Mach RL, de Graaff LH.** 2008. Regulation of transcription of cellulases- and hemicellulases-encoding genes in *Aspergillus niger* and *Hypocrea jecorina* (*Trichoderma reesei*). Appl Microbiol Biotechnol **78:** 211–220. http://dx.doi.org/10.1007/s00253-007-1322-0.
42. **Gielkens MM, Dekkers E, Visser J, de Graaff LH.** 1999. Two cellobiohydrolase-encoding genes from *Aspergillus niger* require D-xylose and the xylanolytic transcriptional activator XlnR for their expression. Appl Environ Microbiol **65:**4340–4345.
43. **Tani S, Kawaguchi T, Kobayashi T.** 2014. Complex regulation of hydrolytic enzyme genes for cellulosic biomass degradation in filamentous fungi. Appl Microbiol Biotechnol **98:**4829–4837. http://dx.doi.org/10.1007/s00253-014-5707-6.
44. **Cai P, Gu R, Wang B, Li J, Wan L, Tian C, Ma Y.** 2014. Evidence of a critical role for cellodextrin Transporte 2 (CDT-2) in both cellulose and hemicellulose degradation and utilization in *Neurospora crassa*. PLoS One **9:**e89330. http://dx.doi.org/10.1371/journal.pone.0089330.
45. **Li X, Yu VY, Lin Y, Chomvong K, Estrela R, Park A, Liang JM, Znameroski EA, Feehan J, Kim SR, Jin Y, Glass NL, Cate JH.** 2015. Expanding xylose metabolism in yeast for plant cell wall conversion to biofuels. Elife **4:**05896. http://dx.doi.org/10.7554/eLife.05896.
46. **Smith KM, Sancar G, Dekhang R, Sullivan CM, Li S, Tag AG, Sancar C, Bredeweg EL, Priest HD, McCormick RF, Thomas TL, Carrington JC, Stajich JE, Bell-Pedersen D, Brunner M, Freitag M.** 2010. Transcription factors in light and circadian clock signaling networks revealed by genomewide mapping of direct targets for *Neurospora* white collar complex. Eukaryot Cell **9:**1549–1556. http://dx.doi.org/10.1128/EC.00154-10.
47. **Talora C, Franchi L, Linden H, Ballario P, Macino G.** 1999. Role of a white collar-1-white collar-2 complex in blue-light signal transduction. EMBO J **18:**4961–4968. http://dx.doi.org/10.1093/emboj/18.18.4961.
48. **Dunlap JC, Loros JJ.** 2006. How fungi keep time: circadian system in Neurospora and other fungi. Curr Opin Microbiol **9:**579–587. http://dx.doi.org/10.1016/j.mib.2006.10.008.
49. **Schmoll M, Franchi L, Kubicek CP.** 2005. Envoy, a PAS/LOV domain protein of *Hypocrea jecorina* (anamorph *Trichoderma reesei*), modulates cellulase gene transcription in response to light. Eukaryot Cell **4:**1998–2007. http://dx.doi.org/10.1128/EC.4.12.1998-2007.2005.
50. **Cha J, Zhou M, Liu Y.** 2015. Mechanism of the Neurospora circadian clock, a FREQUENCY-centric view. Biochemistry **54:**150–156. http://dx.doi.org/10.1021/bi5005624.
51. **Brown NA, Ries LNA, Goldman GH.** 2014. How nutritional status signalling coordinates metabolism and lignocellulolytic enzyme secretion. Fungal Genet Biol **72:**48–63. http://dx.doi.org/10.1016/j.fgb.2014.06.012.
52. **Weirauch M, Yang A, Albu M, Cote AG, Montenegro-Montero A, Drewe P, Najafabadi H, Lambert S, Mann I, Cook K, Zheng H, Goity A, van Bakel H, Lozano J, Galli M, Lewsey MG, Huang E, Mukherjee T, Chen X, Reece-Hoyes J, Govindarajan S, Shaulsky G, Walhout AJ, Bouget FY, Ratsch G, Larrondo LF, Ecker JR, Hughes TR.** 2014. Determination and inference of eukaryotic transcription factor sequence specificity. Cell **158:**1431–1443. http://dx.doi.org/10.1016/j.cell.2014.08.009.
53. **Traven A, Jelicic B, Sopta M.** 2006. Yeast Gal4: a transcriptional paradigm revisited. EMBO Rep **7:**496–499. http://dx.doi.org/10.1038/sj.embor.7400679.
54. **McCluskey K.** 2003. The Fungal Genetics Stock Center: from molds to molecules. Adv Appl Microbiol **52:**245–262. http://dx.doi.org/10.1016/S0065-2164(03)01010-4.
55. **Colot HV, Park G, Turner GE, Ringelberg C, Crew CM, Litvinkova L, Weiss RL, Borkovich KA, Dunlap JC.** 2006. A high-throughput gene knockout procedure for Neurospora reveals functions for multiple transcription factors. Proc Natl Acad Sci U S A **103:**10352–10357. http://dx.doi.org/10.1073/pnas.0601456103.
56. **Zhang Y, Liu T, Meyer CA, Eeckhoute J, Johnson DS, Bernstein BE, Nussbaum C, Myers RM, Brown M, Li W, Liu XS.** 2008. Model-based analysis of ChIP-Seq (MACS). Genome Biol **9:**R137. http://dx.doi.org/10.1186/gb-2008-9-9-r137.
57. **Quinlan AR, Hall IM.** 2010. BEDTools: a flexible suite of utilities for comparing genomic features. Bioinformatics **26:**841–842. http://dx.doi.org/10.1093/bioinformatics/btq033.
58. **Machanick P, Bailey TL.** 2011. MEME-ChIP: motif analysis of large DNA datasets. BioInformatics **27:**1696–1697. http://dx.doi.org/10.1093/bioinformatics/btr189.
59. **Cline MS, Smoot M, Cerami E, Kuchinsky A, Landys N, Workman C, Christmas R, Avila-Campilo I, Creech M, Gross B, Hanspers K, Isserlin R, Kelley R, Killcoyne S, Lotia S, Maere S, Morris J, Ono K, Pavlovic V, Pico AR, Vailaya A, Wang PL, Adler A, Conklin BR, Hood L, Kuiper M, Sander C, Schmulevich I, Schwikowski B, Warner GJ, Ideker T, Bader GD.** 2007. Integration of biological networks and gene expression data using cytoscape. Nat Protoc **2:**2366–2382. http://dx.doi.org/10.1038/nprot.2007.324.